Stem Cell Reports, Volume *8*

Supplemental Information

Bone Size and Quality Regulation: Concerted Actions of mTOR in Mesenchymal Stromal Cells and Osteoclasts

Hongguang Wu, Zhixiang Wu, Ping Li, Qian Cong, Rongrong Chen, Wenrui Xu, Soma Biswas, Huijuan Liu, Xuechun Xia, Shanshan Li, Weiwei Hu, Zhenlin Zhang, Samy L. Habib, Lingli Zhang, Jun Zou, Hongbing Zhang, Weihong Zhang, and Baojie Li

Figure S1

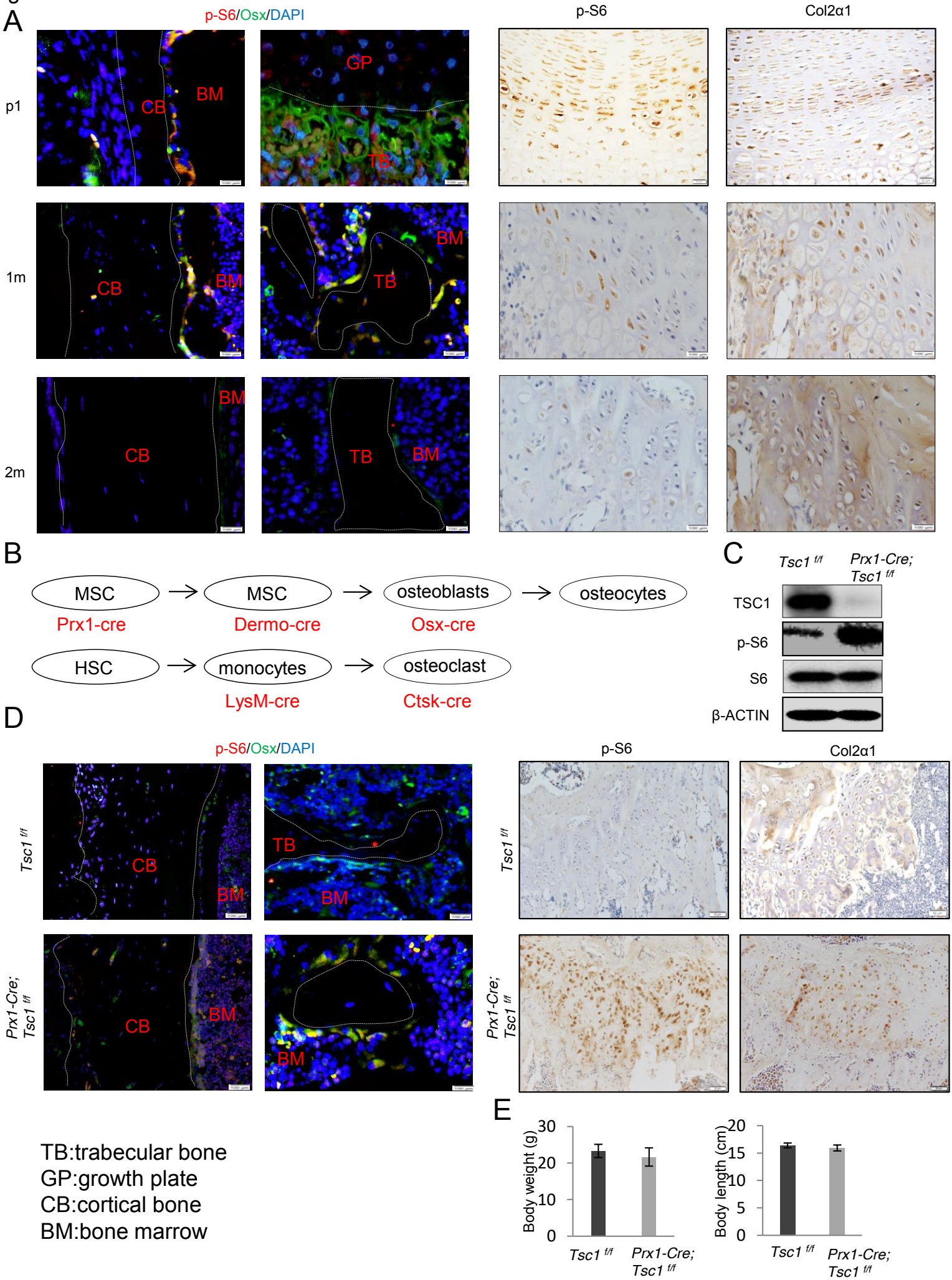

TB:trabecular bone
GP:growth plate
CB:cortical bone
BM:bone marrow

Figure S2

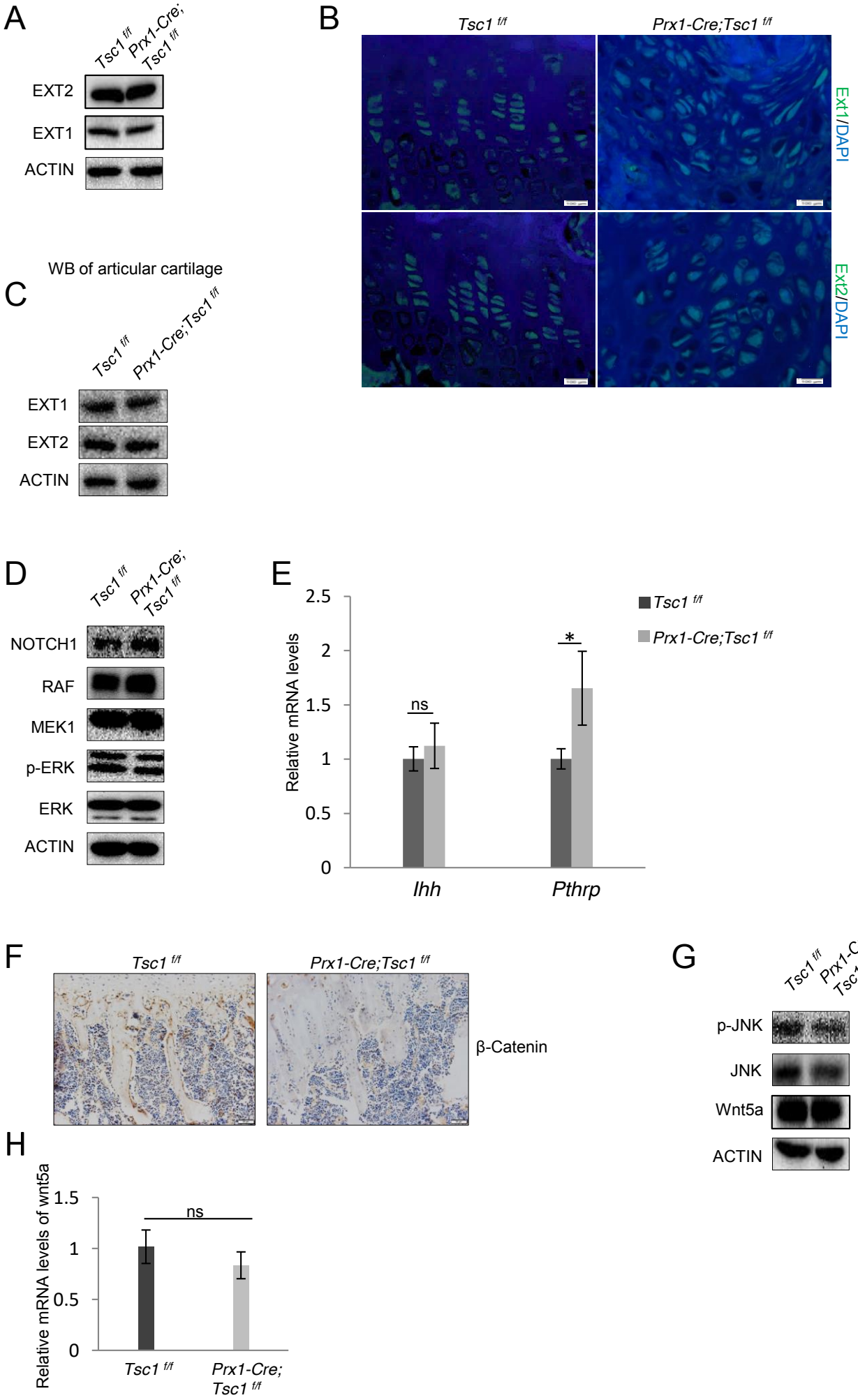
A
Tsc1 f/f
Prx1-Cre; Tsc1 f/f
EXT2
EXT1
ACTIN
B
Tsc1 f/f
Prx1-Cre;Tsc1 f/f
Ext1/DAPI
Ext2/DAPI
WB of articular cartilage
C
Tsc1 f/f
Prx1-Cre;Tsc1 f/f
EXT1
EXT2
ACTIN
D
Tsc1 f/f
Prx1-Cre; Tsc1 f/f
NOTCH1
RAF
MEK1
p-ERK
ERK
ACTIN
E
Relative mRNA levels
2.5
2
1.5
1
0.5
0
ns
*
Tsc1 f/f
Prx1-Cre;Tsc1 f/f
Ihh
Pthrp
F
Tsc1 f/f
Prx1-Cre;Tsc1 f/f
β-Catenin
G
Tsc1 f/f
Prx1-Cre; Tsc1 f/f
p-JNK
JNK
Wnt5a
ACTIN
H
Relative mRNA levels of wnt5a
1.5
1
0.5
0
ns
Tsc1 f/f
Prx1-Cre; Tsc1 f/f

Figure S3

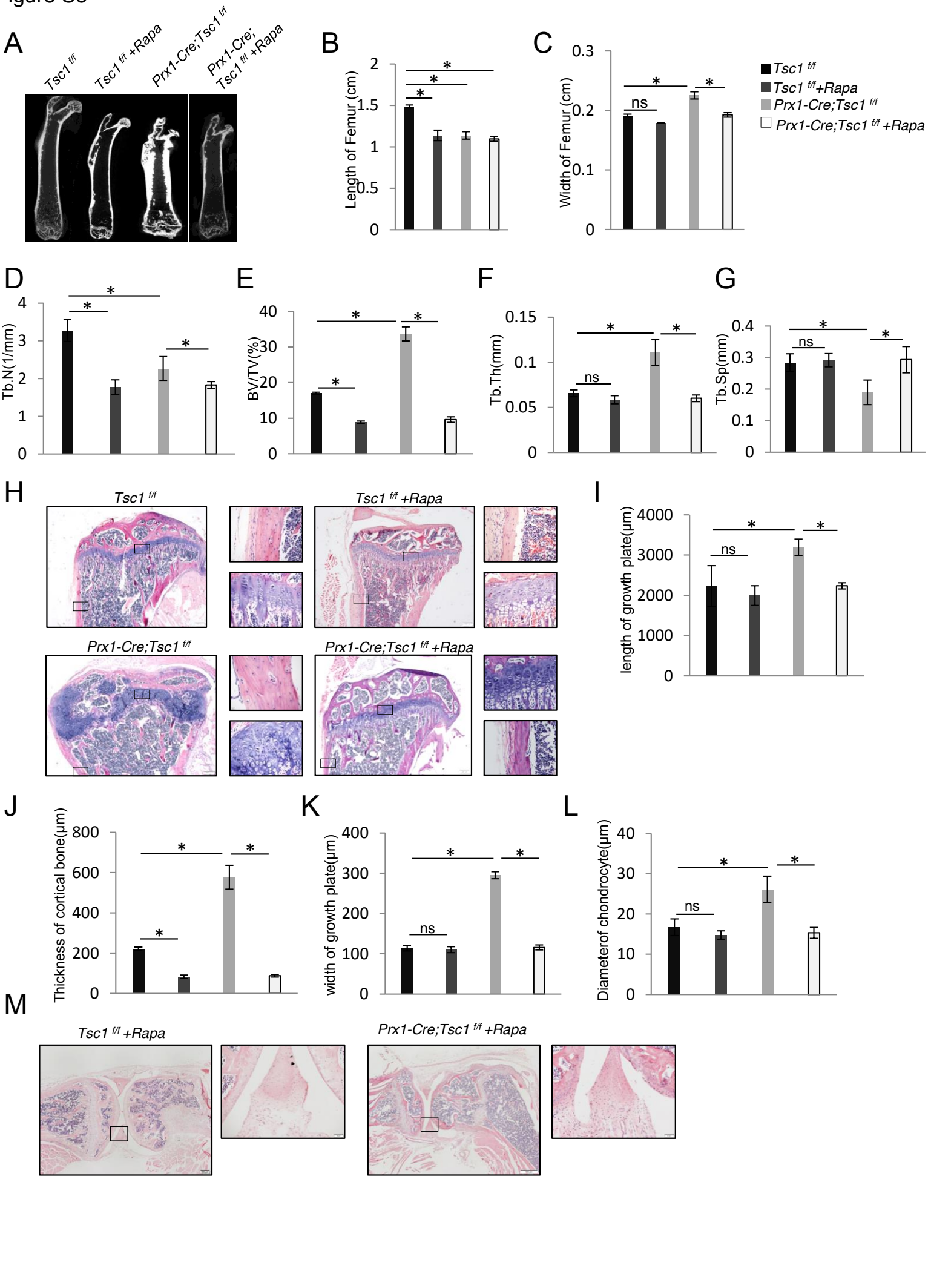
A
Tsc1 f/f
Tsc1 f/f +Rapa
Prx1-Cre;Tsc1 f/f
Prx1-Cre; Tsc1 f/f +Rapa
B
Length of Femur (cm)
C
Width of Femur (cm)
ns
Tsc1 f/f
Tsc1 f/f+Rapa
Prx1-Cre;Tsc1 f/f
Prx1-Cre;Tsc1 f/f +Rapa
D
Tb.N(1/mm)
E
BV/TV(%)
F
Tb.Th(mm)
G
Tb.Sp(mm)
H
Tsc1 f/f
Tsc1 f/f +Rapa
Prx1-Cre;Tsc1 f/f
Prx1-Cre;Tsc1 f/f +Rapa
I
length of growth plate(μm)
J
Thickness of cortical bone(μm)
K
width of growth plate(μm)
L
Diameterof chondrocyte(μm)
M
Tsc1 f/f +Rapa
Prx1-Cre;Tsc1 f/f +Rapa

Figure S4

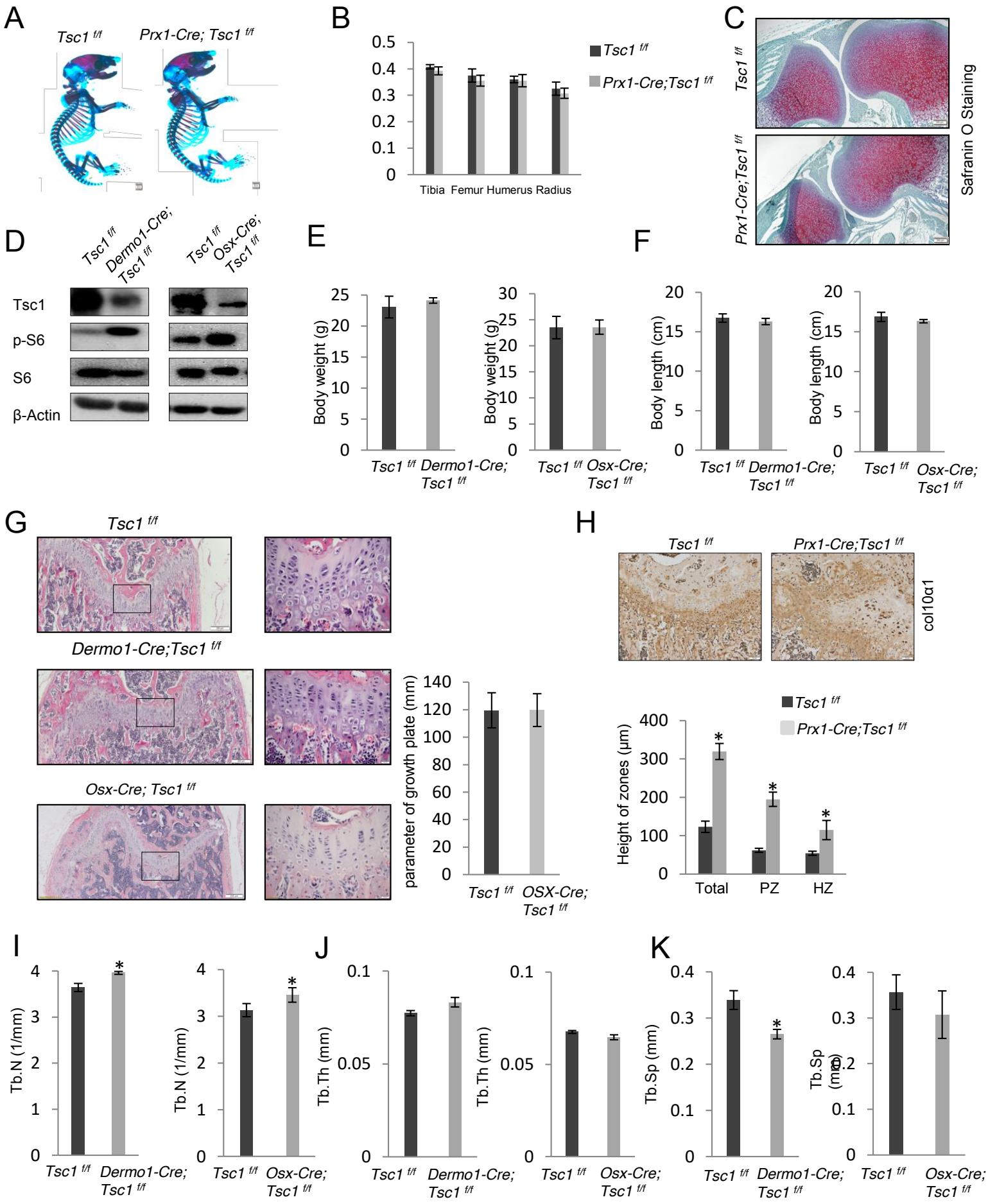
A
Tsc1 f/f
Prx1-Cre; Tsc1 f/f
B
Tsc1 f/f
Prx1-Cre;Tsc1 f/f
Tibia Femur Humerus Radius
C
Tsc1 f/f
Prx1-Cre;Tsc1 f/f
Safranin O Staining
D
Tsc1 f/f Dermo1-Cre; Tsc1 f/f
Tsc1 f/f Osx-Cre; Tsc1 f/f
Tsc1
p-S6
S6
β-Actin
E
Body weight (g)
Tsc1 f/f Dermo1-Cre; Tsc1 f/f
Tsc1 f/f Osx-Cre; Tsc1 f/f
F
Body length (cm)
Tsc1 f/f Dermo1-Cre; Tsc1 f/f
Tsc1 f/f Osx-Cre; Tsc1 f/f
G
Tsc1 f/f
Dermo1-Cre;Tsc1 f/f
Osx-Cre; Tsc1 f/f
parameter of growth plate (mm)
Tsc1 f/f OSX-Cre; Tsc1 f/f
H
Tsc1 f/f
Prx1-Cre;Tsc1 f/f
col10α1
Tsc1 f/f
Prx1-Cre;Tsc1 f/f
Height of zones (μm)
Total PZ HZ
I
Tb.N (1/mm)
Tsc1 f/f Dermo1-Cre; Tsc1 f/f
Tsc1 f/f Osx-Cre; Tsc1 f/f
J
Tb.Th (mm)
Tsc1 f/f Dermo1-Cre; Tsc1 f/f
Tsc1 f/f Osx-Cre; Tsc1 f/f
K
Tb.Sp (mm)
Tsc1 f/f Dermo1-Cre; Tsc1 f/f
Tsc1 f/f Osx-Cre; Tsc1 f/f

Figure S5

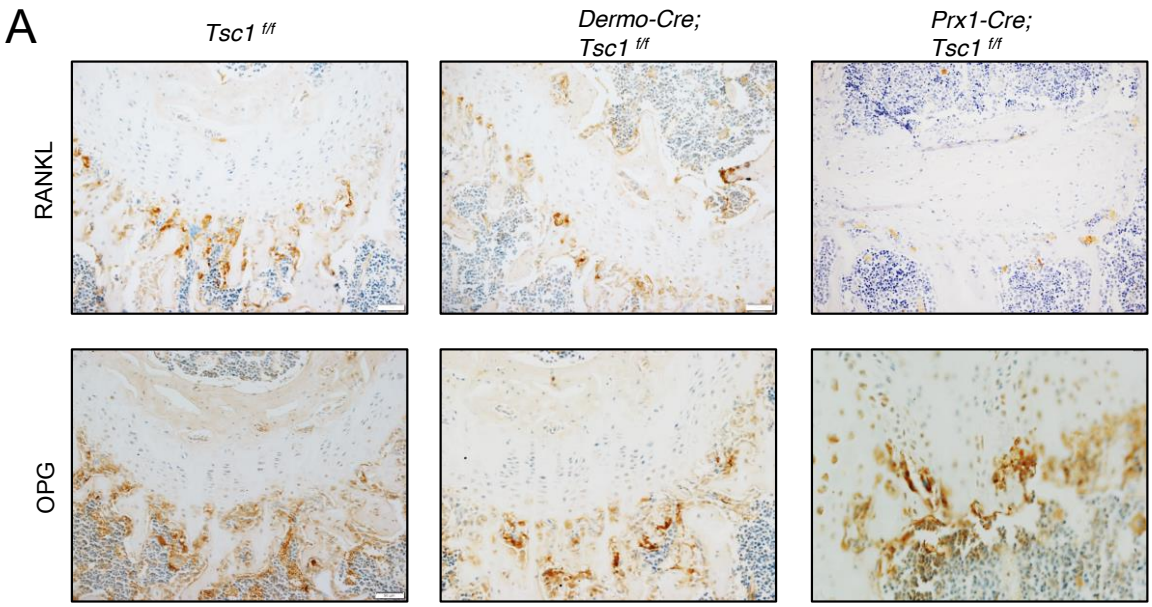
A
Tsc1 f/f
Dermo-Cre; Tsc1 f/f
Prx1-Cre; Tsc1 f/f
RANKL
OPG

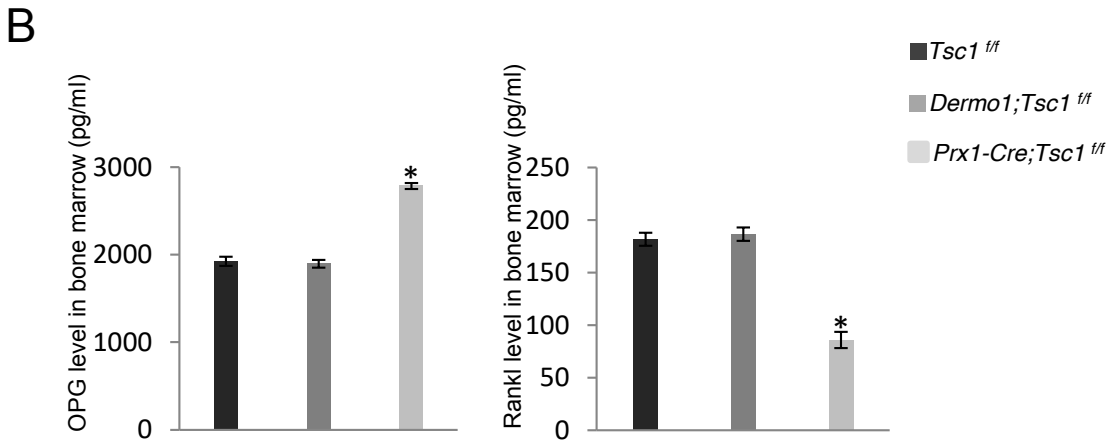
B
OPG level in bone marrow (pg/ml)
3000
2000
1000
0
*
Rankl level in bone marrow (pg/ml)
250
200
150
100
50
0
*
Tsc1 f/f
Dermo1;Tsc1 f/f
Prx1-Cre;Tsc1 f/f

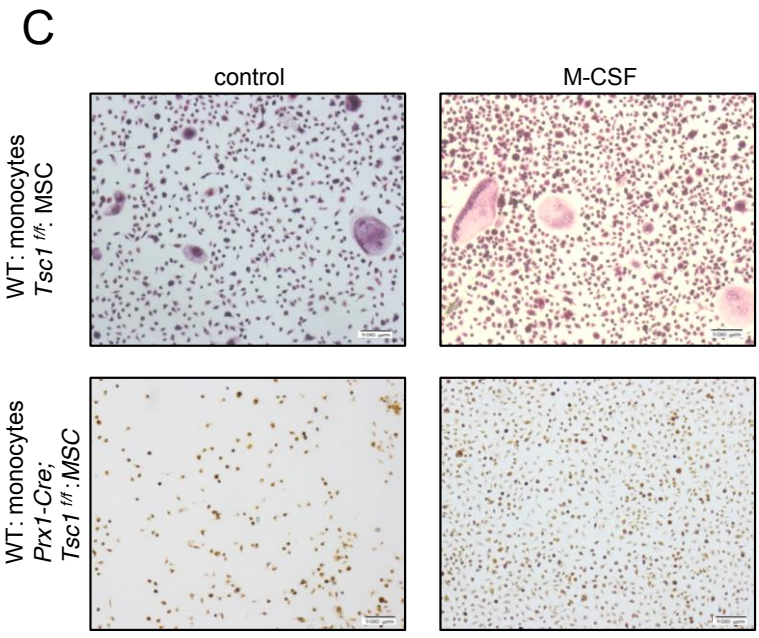
C
control
M-CSF
WT: monocytes
Tsc1 f/f: MSC
WT: monocytes
Prx1-Cre;
Tsc1 f/f :MSC

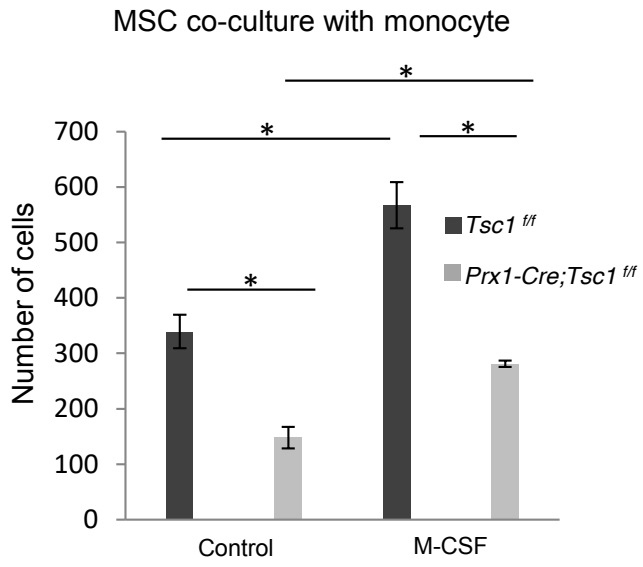
MSC co-culture with monocyte
Number of cells
700
600
500
400
300
200
100
0
*
*
*
*
Tsc1 f/f
Prx1-Cre;Tsc1 f/f
Control
M-CSF

Figure S6

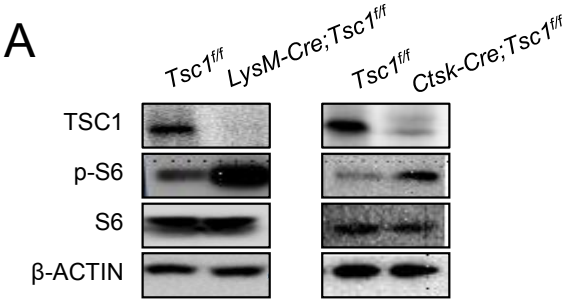
A
Tsc1f/f
LysM-Cre;Tsc1f/f
Tsc1f/f
Ctsk-Cre;Tsc1f/f
TSC1
p-S6
S6
β-ACTIN

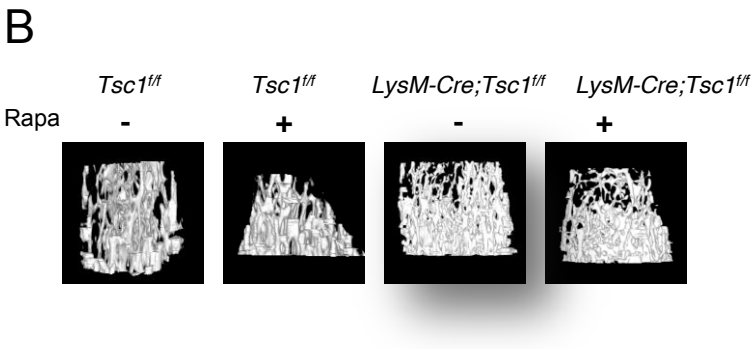
B
Tsc1f/f
Tsc1f/f
LysM-Cre;Tsc1f/f
LysM-Cre;Tsc1f/f
Rapa
-
+
-
+

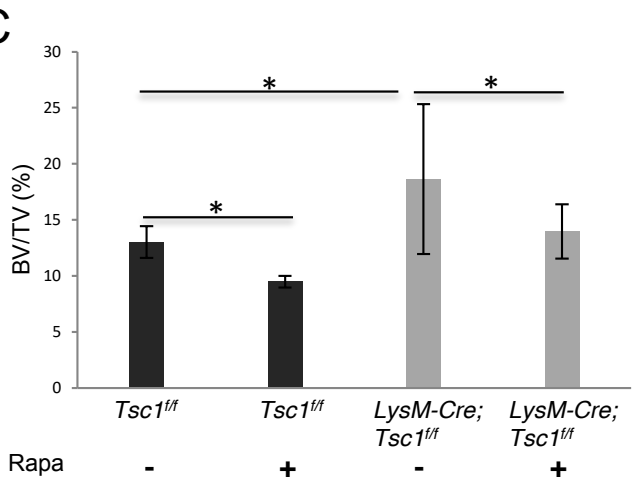
C
BV/TV (%)
30
25
20
15
10
5
0
*
*
*
Tsc1f/f
Tsc1f/f
LysM-Cre; Tsc1f/f
LysM-Cre; Tsc1f/f
Rapa
-
+
-
+

Figure S7

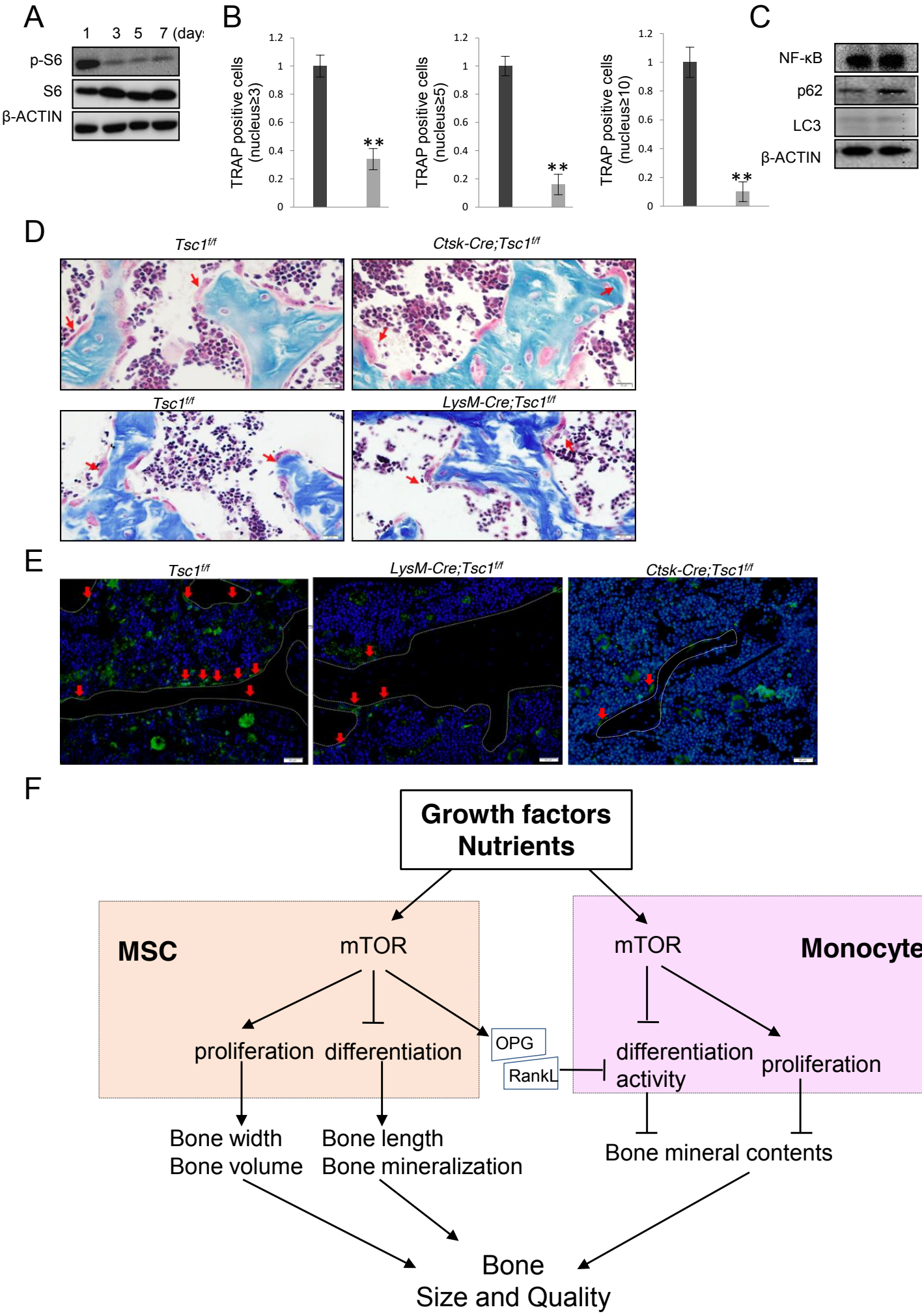
A
1 3 5 7 (day
p-S6
S6
β-ACTIN
B
TRAP positive cells (nucleus≥3)
TRAP positive cells (nucleus≥5)
TRAP positive cells (nucleus≥10)
**
C
NF-κB
p62
LC3
β-ACTIN
D
Tsc1f/f
Ctsk-Cre;Tsc1f/f
Tsc1f/f
LysM-Cre;Tsc1f/f
E
Tsc1f/f
LysM-Cre;Tsc1f/f
Ctsk-Cre;Tsc1f/f
F
Growth factors
Nutrients
MSC
mTOR
proliferation
differentiation
OPG
RankL
mTOR
Monocyte
differentiation activity
proliferation
Bone width
Bone volume
Bone length
Bone mineralization
Bone mineral contents
Bone
Size and Quality

Supplementary Figure legend

Figure S1. Staining of p-S6 and Osx or Col2α on bone sections of *WT* and *Prx1-Cre; Tsc1$^{f/f}$* mice, related to Figure 1.

A. Staining of p-S6 and Osx (left panels) or Col2α (right panels) on bone sections of p1, 1-month-old, and 2-month-old WT mice, showing mTOR activation at growth plate, trabecular bone, and periosteal/endosteal surfaces. Note that the anti-Col2α and p-S6 antibodies are from the same species so we stained them on separate sections. Scale bar, 50 μm.
B. A diagram to show the *Cre* mice that were used to ablate *Tsc1* in different cells along the lines of osteoblast and osteoclast differentiation.
C. Western blot showed that deletion of *Tsc1* led to mTOR activation in BM-MSCs, manifested an increase in p-S6. Scale bar, 50 μm.
D. Staining of p-S6 and Osx (left panels) or Col2α (right panels) on bone sections of *Prx1-Cre; Tsc1$^{f/f}$* and control mice, showing mTOR activation was enhanced in the mutant mice at growth plate, trabecular bone, and periosteal/endosteal surfaces. Scale bar, 50 μm.
E. Normal body weights and body lengths of *Prx1-Cre; Tsc1$^{f/f}$* compared to control male mice at 2.5 month of age. N=15 mice.

Figure S2. The expression and/or activation of mTOR-independent pathway molecules, β-Catenin-independent pathway molecules and Ext1/2, related to Figure 2 and 4.

A. Western blot results showed that the protein levels of EXT1 and EXT2 were unaltered in *Tsc1$^{-/-}$* BM-MSCs compared to control BM-MSCs.
B. Staining of EXT1 and EXT2 on femur bone sections of *Prx1-Cre; Tsc1$^{f/f}$* and WT mice. Scale bar, 50 μm.
C. Western blot results showed that the protein levels of EXT1 and EXT2 were unaltered in *Tsc1$^{-/-}$* femur head cartilage samples compared to control samples.
D. Western blot results showed that NOTCH1 protein levels were increased while

the levels of B-RAF, MEK1, or p-ERK2 were unaltered in *Tsc1*$^{-/-}$ BM-MSCs compared to control BM-MSCs.

E. Quantitative PCR showed that *Tsc1* deletion increased the mRNA levels of *Pthrp* but not *Ihh* in BM-MSCs. The experiments were repeated 3 times with triplicate.

F. Immuno-staining for β-Catenin on femur sections of *Prx1-Cre; Tsc1*$^{f/f}$ and control mice, showing that β-Catenin was decreased on *Prx1-Cre; Tsc1*$^{f/f}$ mouse bones. Scale bar, 50 μm.

G. Western blot results showed that *Tsc1* deletion decreased the activation of JNK without affecting the expression of WNT5a in BM-MSCs.

H. Quantitative PCR showed unaltered mRNA levels of *Wnt5a* in *Tsc1*$^{-/-}$ BM-MSCs compared to control BM-MSCs. The experiments were repeated 3 times with triplicate.

Figure S3. Rapamycin treatment largely rescued the histomorphometry indices and the growth plate and joint defects of *Prx1-Cre; Tsc1*$^{f/f}$ mice, related to Figure 2 and 3. Rapamycin was intraperitoneally injected into 3-week-old mutant and control mice at the dose of 3 μg/g body weight per day for 40 days. N=5 mice.

A. Micro-CT images of the femurs of rapamycin (rapa) or solvent-treated *Tsc1*$^{f/f}$ and *Prx1-Cre; Tsc1*$^{f/f}$ mice.

B. The femur length of rapamycin or solvent-treated *Tsc1*$^{f/f}$ and *Prx1-Cre; Tsc1*$^{f/f}$ mice.

C. The femur width of rapamycin or solvent-treated *Tsc1*$^{f/f}$ and *Prx1-Cre; Tsc1*$^{f/f}$ mice.

D. The number of trabecular bones of rapamycin or solvent-treated *Tsc1*$^{f/f}$ and *Prx1-Cre; Tsc1*$^{f/f}$ mice.

E. The BV/TV of rapamycin or solvent-treated *Tsc1*$^{f/f}$ and *Prx1-Cre; Tsc1*$^{f/f}$ mice.

F. The thickness of the trabecular bones of rapamycin or solvent-treated *Tsc1*$^{f/f}$ and *Prx1-Cre; Tsc1*$^{f/f}$ mice.

G. The separation of trabecular bones of rapamycin or solvent-treated *Tsc1*$^{f/f}$ and

Prx1-Cre; Tsc1$^{f/f}$ mice.

H. H/E staining of the decalcified femur growth plates of rapamycin or solvent-treated *Tsc1*$^{f/f}$ and *Prx1-Cre; Tsc1*$^{f/f}$ mice. Scale bar, 200 μm.

I. The length of the femur growth plate of rapamycin or solvent-treated *Tsc1*$^{f/f}$ and *Prx1-Cre; Tsc1*$^{f/f}$ mice.

J. The thickness of the femur cortical bones of rapamycin or solvent-treated *Tsc1*$^{f/f}$ and *Prx1-Cre; Tsc1*$^{f/f}$ mice.

K. The width of the growth plates of rapamycin or solvent-treated *Tsc1*$^{f/f}$ and *Prx1-Cre; Tsc1*$^{f/f}$ mice.

L. The diameter of the chondrocytes of rapamycin or solvent-treated *Tsc1*$^{f/f}$ and *Prx1-Cre; Tsc1*$^{f/f}$ mice.

M. H/E staining of the joints of rapamycin or solvent-treated *Tsc1*$^{f/f}$ and *Prx1-Cre; Tsc1*$^{f/f}$ mice. Scale bar, 200 μm.

Figure S4. The phenotypes of *Prx1-Cre; Tsc1*$^{f/f}$ embryos and p1 pups and *Dermo1-Cre; Tsc1*$^{f/f}$ and *Osx-Cre; Tsc1*$^{f/f}$ adult mice, related to Figure 2 and 5.

A. The *Prx1-Cre; Tsc1*$^{f/f}$ E18.5 embryo skeleton appeared to be normal. The mutant and control embryos were stained with alizarin red and alcian blue. Scale bar, 200 μm.

B. The long bones of p1 *Prx1-Cre; Tsc1*$^{f/f}$ were similar in length as the control pups. N=4 mice.

C. H/E staining revealed that the *Prx1-Cre; Tsc1*$^{f/f}$ p1 pups showed normal joint. Scale bar, 200 μm.

D. Western blot showed that Tsc1 was deleted in the BM-MSCs of *Dermo1-Cre; Tsc1*$^{f/f}$ mice (left panel) and osteoblasts of *Osx-Cre; Tsc1*$^{f/f}$ mice (right panel). BM-MSCs were isolated from *Osx-Cre; Tsc1*$^{f/f}$ and were induced to differentiate into osteoblasts by 50 ng/ml of BMP2 for 5 days. The cells were collected and the cell samples were analyzed by western blot.

E. Normal body weights of *Dermo1-Cre; Tsc1*$^{f/f}$ mice (left panel) and *Osx-Cre; Tsc1*$^{f/f}$ mice (right panel) compared to their controls. N=4 mice.

F. Normal body lengths of *Dermo1-Cre; Tsc1$^{f/f}$* mice (left panel) and osteoblasts of *Osx-Cre; Tsc1$^{f/f}$* mice (right panel). N=4 mice.

G. HE staining of femur bones revealed that *Dermo1-Cre; Tsc1$^{f/f}$* mice (left panel) and *Osx-Cre; Tsc1$^{f/f}$* mice (right panel) showed normal growth plates. The right panel: the heights of the growth plates of *Osx-Cre; Tsc1$^{f/f}$* and control mice. Scale bars, 200 μm (left panel) and 50 μm (middle panel). N=3 mice

H. Immuno-staining for Col10 on femur sections of *Prx1-Cre; Tsc1$^{f/f}$* and control mice (upper panel). Bottom panel: quantitation data for the heights of the proliferation zone (PZ) (based on Fig. 4A) and hypertrophic zone (HZ) (based on Col10) and the total growth plate zone (based on Fig. S3H). Scale bar, 50 μm. N=3 mice

I. Trabecular bone numbers were increased in *Dermo1-Cre; Tsc1$^{f/f}$* mice and *Osx-Cre; Tsc1$^{f/f}$* mice. N=4 mice.

J. Trabecular bone thickness was not significantly altered in *Dermo1-Cre; Tsc1$^{f/f}$* mice or *Osx-Cre; Tsc1$^{f/f}$* mice. N=4 mice.

K. Trabecular bone separation was decreased in *Dermo1-Cre; Tsc1$^{f/f}$* mice. N=4 mice.

Figure. S5. *Prx1-Cre; Tsc1$^{f/f}$* mouse bones showed altered expression of *Rankl* and *Opg*. N=3 mice.

A. Immunohistochemistry staining for RANKL and OPG on femur sections of *Prx1-Cre; Tsc1$^{f/f}$*, *Dermo-Cre; Tsc1$^{f/f}$* and control mice, showing that RANKL was decreased whereas OPG was increased on *Prx1-Cre; Tsc1$^{f/f}$* mouse bones. Scale bar, 50 μm.

B. *Prx1-Cre; Tsc1$^{f/f}$* mouse bone marrow showed an increase in OPG and a decrease in RANKL levels. Femur and tibia bones were used for the assay. N=3 independent experiments.

C. Co-culture experiments showed that reduced synthesis of M-CSF by *Tsc1$^{-/-}$* MSCs compromised the proliferation of monocytes. *Tsc1$^{-/-}$* or WT MSCs were plated overnight and then normal monocytes were plated on top of the MSCs. These plates were treated with M-CSF (25 ng/ml) for 3 days and the pictures were taken

under microscope. Right panel: Quantitation data of total cells of 5 random views of three repeated results. Scale bar, 50 μm. N=3 independent experiments.

Figure S6. Rapamycin treatment largely rescued the bone mass phenotype of *LysM-Cre; Tsc1*$^{f/f}$ mice, related to Fig. 6.

Rapamycin was intraperitoneally injected into 3 week-old mutant and control mice at the dose of 3 μg/g body weight per day for 40 days. N=5 mice.

A. Western blot showed deletion of *Tsc1* led to mTOR activation in *LysM*+ monocytes (left panel) and *Ctsk*+ osteoclasts (right panel), leading to an increase in p-S6.
B. Micro-CT images of the femur bones of rapamycin (rapa) or solvent-treated *Tsc1*$^{f/f}$ and *LysM-Cre; Tsc1*$^{f/f}$ mice.
C. The BV/TV of femurs of rapamycin or solvent-treated *Tsc1*$^{f/f}$ and *LysM-Cre; Tsc1*$^{f/f}$ mice.

Figure S7. *Tsc1* ablation inhibited osteoclast differentiation and resorption activity by altering OC size and the number of actin ring-like structures, related to Fig. 6 and 7.

A. mTOR activation was suppressed when monocytes were induced to differentiate into osteoclasts by M-CSF and RANKL.
B. Deletion of *Tsc1* in *LysM*+ monocytes impeded osteoclast differentiation. WT and *Tsc1*$^{-/-}$ monocytes were induced to differentiate by M-CSF and RANKL. After 5 days, the number of nuclei in each TRAP positive cells were counted and presented. The experiments were repeated 5 times with 3 mice each.
C. *Tsc1*$^{-/-}$ osteoclasts showed normal levels of autophagy markers p62 and LC3.
D. The abnormal morphology of the osteoclasts on bone sections of *Ctsk-Cre; Tsc1*$^{f/f}$ and *LysM-Cre; Tsc1*$^{f/f}$ mice (upper panel) whereas osteoclasts looked normal in *LysM-Cre; Tsc1*$^{f/f}$mice (upper panel). Scale bar, 50 μm.
E. *LysM-Cre; Tsc1*$^{f/f}$ (left panel) and *Ctsk-Cre; Tsc1*$^{f/f}$mouse (right panel) femur sections showed a decrease in the number of actin ring-like structures at the bone surface. Scale bar, 50μm.

F. A diagram showing the multiple roles played by mTOR signaling in bone size and quality control.

Supplementary Experimental Procedures

Bone histomorphometry

Bone histomorphometry was performed on undecalcified sections. For dynamic histomorphometric analysis，mice received injections of calcein (20 mg/kg) at 8 and 2d prior to sacrifice. The femur was embedded in methyl methacrylate after dehydration and xylene treatment. Four-μm-thick sections were made using a hard tissue microtome (Leica Microsystems Nussloch GmbH). The sections were left unstained for measurement of double calcein labeling. For bone-specific parameters measurement, the slides were stained with Villanueva-Goldner's trichrome method. Images were taken and analyzed using the Olympus DP72 microscope (Olympus Microsystems). All parameters were measured using OsteoMeasure software (OsteoMetrics).

Bone three-point bending experiment

Three-point bending experiments were conducted on an equipment (Reger RGM-2020, China) using fixed femurs. The ends of the femurs were fixed on the machine pedestal in horizontal position with a 12 mm span. The probe continuously moved down at the speed of 1 mm/min to press the bone, which automatically stopped 1 min after the bone fractured. All the data were collected and analyzed with the software supplied by the manufacturer. Then Vernier caliper was used for measurement of femoral long axis, short axis and minor axis in the central part of trabecular thickness. Max load, yield stress, and elastic modulus were automatically calculated by the software provided by the manufacturer.

X-ray and micro-CT analysis

The whole-body and femurs radiographs were taken with the Cabinet X-Ray system (LX-60, Faxitron Bioptics) using a standardized setting (45Kv for 8s). Trabecular and cortical bone architecture were assessed in femurs employing a micro-computed tomography analysis (micro-CT) system (micro-CT 40, Scanco Medical) performed following protocols provided by the manufacturer.

Isolation and culture of BM-MSCs

Mice of 6-8 weeks of age were sacrificed by cervical dislocation, rinsed in 70%

(vol/vol) ethanol for 3 min. The femur and tibia bones were extracted and cleaned free of muscle. The bones were placed in a dish of sterile PBS on ice. The femur or tibia ends were cut and the bone marrow was flushed out with α-MEM using a syringe. This was repeated a few times until the bone looked pale. The cells were dispersed and filtered through a 70 μm mesh to remove any bone debris. The BM-MSCs were cultured in α-MEM containing 15% (vol/vol) FBS in the presence of 100 μg/ml penicillin and 100 μg/ml streptomycin at 37℃ with 5% CO_2 in a humidified chamber for 5 days. Then the nonadherent cells were washed out with PBS and the BM-MSCs were either directly used or frozen for future experiments.

Differentiation of BM-MSCs

For MSC differentiation assays, BM-MSCs were seeded at a density of $5x10^4$ cells/well in 12-well plates with complete medium. The next day, the cells were cultured in complete medium supplemented with 10 mM β-glycerol phosphate and 50 μg/ml ascorbic acid for 7-10 days, with the medium changed every 3 days. The cells were then washed with PBS, fixed in 4% paraformaldehyde for 30 min, and stained for ALP using an Alkaline Phosphatase Kit (Sigma) following the manufacturer's instructions. For mineralization assay, the cells were cultured for 14, 21, or 28 days, which were then rinsed with distilled water, stained in 5% (wt/vol) silver nitrate solution under ultraviolet light for 1h, washed three times with distilled water, and then added 500 μl 5% (wt/vol) sodium thiosulfate solution to stop the reaction.

For MSC adipocyte differentiation, MSCs were plated at a density of $1x10^5$ cells/well in a 12-well plate and cultured in α-MEM supplemented with 15% FBS, 100 nM dexamethasone, and 5 μM insulin for 2 weeks. The cells were then washed, fixed in 4% paraformaldehyde for 30 min, and stained with Oil-red-O solution. For chondrocyte differentiation, MSCs were seeded at a density of 1.6×10^7 cells/well in 5 μl droplets in the center of wells in a 12-well plate, cultured at in α-MEM supplemented with 15% FBS, 100 nM dexamethasone, 10 ng/ml TGF-β1，and 1 μM ascorbate-2-phosphate for 21 days. The cells were then washed with PBS, fixed in 4% paraformaldehyde for 30 min, and stained with 1% Alcian Blue solution (in 0.1N HCL) for 30min.

Isolation and differentiation of monocytes

The bone marrow cells were cultured in α-MEM containing 15% (vol/vol) FBS in the presence of 100 μg/ml penicillin and 100 μg/ml streptomycin) at 37℃ with 5% CO2 in a humidified chamber for 16 hrs. The nonadherent cells were harvested and seeded at a density of $1x10^6$ cells/well in a 96-well plate for TRAP staining or at a density of 3×10^7 cells/well in two 6-well plates to collect RNA and Protein. These cells were cultured in α-MEM containing M-CSF (50 ng/ml) and RANKL (100 ng/ml) for 5 days, and stained for TRAP using a TRAP-leukocyte kit (sigma).

TRAP staining

To stain osteoclast cultures after BM monocytes were induced to differentiate with RANKL and M-CSF, the cells were fixed in 4% PBS-buffered paraformaldehyde for 30 min, washed with PBS, and then stained with Leukocyte Acid Phosphatase kit (387A, Sigma-Aldrich) for 1h at 37 °C, following the manufacturer's instructions. Images were taken and analyzed using the Olympus DP72 microscope (Olympus Microsystems). TRAP+ multinucleated cells (>3 nuclei) were counted as osteoclasts.

To stain bone sections, tibiae and femur were dissected out, fixed in 4% PBS-buffered paraformaldehyde overnight at 4 °C, decalcified in 15% EDTA for 2 weeks and washed with distilled water. The samples were dehydrated in gradient alcohols, cleared with xylene, embedded in paraffin through the standard procedures. Four-μm-thick sections were cut using microtome (Lexica Microsystems Nussle GmbH). the bone sections were deparaffinized in xylene and rehydrated in gradient alcohols. The slides were then stained with the Leukocyte Acid Phosphatase kit (387A, Sigma-Aldrich) for 1h at 37°C according to the manufacturer's instructions. Images were taken using the Olympus DP72 microscope (Olympus Microsystems).

Resorption pit analysis

Bone marrow monocytes were induced to differentiate into osteoclasts in the presence of RANKL and M-CSF for 3 days. These differentiated osteoclasts were trypsinized off the plates and seeded onto the dentin slices for 5 more days. The dentin slices were washed with PBS and fixed in 2.5% glutaraldehyde, sonicated in 1N NaOH for 1 minute to remove cells, and stained with 1% toluidine blue solution

for 10 min at room temperature. Resorption pits on bone slice were observed and numbered in 20 random fields of vision under a microscope.

Quantitative PCR

Total RNA was extracted by using Trizol regent (invitrogen). The RNA was reverse transcribed using Transcriptor Universal cDNA Master (Roche) according to the manufacturer's instructions. Real-time PCR was performed using Fast Start Universal SYBR Green Master kit (Roche) using ABI Prism 7500 Sequence Detection System (Applied Biosystems). The relative levels of mRNA species were calculated using the delta-delta CT method. The expression of all the target genes was normalized to *GAPDH*. The primer sequences are listed below:

Pparγ Forward:5'-GGAAAGACAACGGACAAATCAC-3' Reverse:5'-TACGGATCGAAACTGGCAC-3'

Col1a1 Forward:5'-CCGGAAGAATACGTATCACC-3' Reverse:5'-ACCAGGAGGACCAGGAAGTC-3'

Osterix Forward:5'-TGAGGAAGAAGCCCATTCAC-3' Reverse:5'-ACTTCTTCTCCCGGGTGTG-3'

Runx2 Forward:5'-CCGGTCTCCTTCCAGGAT-3' Reverse:5'-GGGAACTGCTGTGGCTTC-3'

RankL Forward:5'-GGGAACTGCTGTGGCTTC-3' Reverse:5'-GATGGTGAGGTGTGCAAATG-3'

Opg Forward:5'-AGCTGCTGAAGCTGTGGAA-3' Reverse:5'-GGTTCGAGTGGCCGAGAT-3'

M-Csf Forward:5'-GGAGACCTCGTGCCAAATTA-3' Reverse:5'-TATCTCTGAAGCGCAAGGTG-3'

Sox9 Forward:5'-GGAGCTCGAAACTGACTGGAA-3' Reverse:5'-GAGGCGAATTGGAGAGGAGGA-3'

E-Cadherin Forward:5'-TCAGTTCCGAGGTCTACAC-3' Reverse:5'-CTTCAAATCTCACTCTGCCC-3'

DC-Stamp Forward:5'-TACGTGGAGAGAAGCAAGGAA-3' Reverse:5'-ACACTGAGACGTGGTTTAGGAAT-3

OC-Stamp Forward:5'-TGGGCCTCCATATGACCTCGAGTAG-3 Reverse:5'-TCAAAGGCTTGTAAATTGGAGGAGT-3'

Nfatc1 Forward:5'-TGGAGAAGCAGAGCACAGAC-3' Reverse:5'-GCGGAAAGGTGGTATCTCAA-3'

C-Fos Forward:5'-CGGGTTTCAACGCCGACTA-3' Reverse:5'-TTGGCACTAGAGACGGACAGA-3'

Actin Forward:5'-CGTGAAAAGATGACCCAGATCA-3' Reverse:5'-CACAGCCTGGATGGCTACGT-3'

Mmp9 Forward 5'-CTGGACAGCCAGACACTAAAG-3' Reverse 5'-CTCGCGGCAAGTCTTCAGAG-3'

Ctsk Forward 5'-GAAGAAGACTCACCAGAAGCAG -3' Reverse 5'-TCCAGGTTATGGGCAGAGATT-3'

Trap Forward 5'-TGTCATCTGTGAAAAGGTGGTC-3' Reverse 5'-ACTGGAGCAGCGGTGTTATG-3'

Ihh Forward 5'-CTCTTGCCTACAAGCAGTTCA-3' Reverse 5'-CCGTGTTCTCCTCGTCCTT-3'

Pthrp Forward 5'-CATCAGCTACTGCATGACAAGG-3' Reverse 5'-GGTGGTTTTTGGTGTTGGGAG-3'

Wnt5a Forward 5'-CAACTGGCAGGACTTTCTCAA-3' Reverse 5'-CATCTCCGATGCCGGAACT-3'

Immunohistochemical staining

Bone sections were deparaffinized in xylene and rehydrated in gradient alcohols, then permeabilized with 0.1% Triton X-100 for 20 min at room temperature. Antigen retrieval was performed in citrate buffer. After that, the slides were blocked with 1% goat serum (dissolved in PBS) for 20 mins, followed by addition of specific primary antibody overnight at 4°C. The next day, the slides were washed in PBS, incubated in

secondary antibody for 1h at 37°C, and washed in PBS before mounted. Images were taken and analyzed using the Olympus DP72 microscope (Olympus Microsystems). Anti-Ki67 (ab15580, Abcam) and p-S6 (CST, 2211l) antibodies were used in this study. Col2α1 (ab-196619) and Col10 (ab58632) antibodies were purchased from Abcam. Osterix antibodies (sc-393325), β-Catenin (sc-7199), Ext1 (sc-515144), and Ext2 (sc-514092) were purchased from Santa Cruz.

Western Blot

Total proteins were extracted from cells or tissues with TNEN buffer containing phosphatase and proteinase inhibitors. Total protein content was determined by the Bradford method (Bio-Rad assay). The samples were then subjected to sodium dodecyl sulfate-polyacrylamide gel electrophoresis (SDS-PAGE) followed by transfer onto nitrocellulose membranes. The proteins were detected with specific antibodies. Immunoreactivity was detected using a Western Chemiluminescent HRP Substrate Kit (Millipore). Membranes were imaged with FluorChem M system (Protein Simple). Antibodies against p-S6 (4587s), p-p38 (9211s), p38 (9212s), Smad4 (9515), p-Smad1 (9553s), Smad1 (9743s), NF-κB (4764s), p-Jnk (9251s), Jnk (9252), and p62 (8025s) were purchased from Cell Signaling Technology, and antibodies against β-Catenin (sc-7199), IκB (sc-945), Ext1 (sc-515144), Ext2 (sc-514092), Wnt5a (sc-365370), and Actin (sc-81178) were purchased from Santa Cruz.

Measurement of bone marrow OPG and RANKL

The bone marrow was taken from the femur and tibia bones of WT and control mice and was centrifuged for 5 minutes. The supernatant was collected and used to determine the levels of OPG and RANKL. Commercially available mouse OPG ELISA detection kit (BOSTER, EK0481) and RANKL ELISA detection kit (BOSTER, EK0843) were used for the measurements.